Regional Environmental Change (2020) 20: 31
https://doi.org/10.1007/s10113-020-01610-z

ORIGINAL ARTICLE

The relation of climate extremes with global warming in the Mediterranean region and its north versus south contrast

Piero Lionello[1,2] · Luca Scarascia[2]

Received: 25 July 2019 / Accepted: 13 November 2019 / Published online: 26 February 2020

Abstract

This study uses the results of 28 CMIP5 global climate projections to link regional climate extremes in the Mediterranean region to the global mean annual surface temperature change. It shows that global warming will further increase the existing difference in intensity of precipitation and hydrological extremes between north and south Mediterranean areas (SMed and NMed, respectively), while the increase/decrease of warm/cold temperature extremes will be only marginally larger in the SMed. The Simple daily precipitation intensity index (SDII) and the total precipitation during very wet days (R95pTOT) are already larger in the NMed than in the SMed; they will increase with global warming at a rate of approximately 0.1 mm/K and 5 mm/K, respectively, in the NMed, with no significant change in the SMed. The maximum number of consecutive dry days (CDD) is already larger in the SMed than in the NMed and will increase more in the former than in the latter (rates are about 8 days/K and 5 days/K, respectively). Global warming will not affect the difference of maximum number of consecutive wet days (CWD), which is presently larger in the NMed than in the SMed and will decrease at a similar rate (about 0.5 days/K) in both areas. Changes of temperature extremes (warm nights, TN90p, and cold days, TX10p) will be similar in the north and south Mediterranean, though marginally larger in several areas of the SMed than in the NMed. Their increase will be dramatic and with a 4 K global warming almost all nights will be warm and there will be no cold days.

Keywords Mediterranean region · Climate change · Extremes · Precipitation · Temperature · Hydrological cycle

Introduction

The Mediterranean region (MedR) has already been shown to be a region where climate change will imply large changes (e.g., Giorgi and Lionello 2008; Planton et al. 2012; Ulbrich et al, 2012; Lionello and Scarascia 2018). A former study has linked the rate of change of mean climate conditions to the global temperature change (Lionello and Scarascia 2018). It has considered annual and seasonal values of total precipitation, of mean daily maximum and minimum temperature. It has shown that mean temperatures in the Mediterranean region will increase at a rate larger than the global mean temperature, particularly in summer, and that total precipitation will decrease at a rate of about −4%/K per degree of global warming. This study extends these previous results considering indices that describe extremes of the hydrological cycle, intensity of precipitation events, warm and cold daily anomalies. Particularly, it aims at assessing differences of future trends between northern and southern areas of the MedR. This analysis is important for understanding whether climate change may pose different risk levels within this region. In the MedR, contrasting magnitude of future increase of climate extremes among different areas can determine different hazard intensity, which, superimposed to the different level exposure and vulnerability, might result in quite different risks within a small spatial scale. The link between changes of regional extremes and the global surface air temperature change represents information that can be immediately used in climate change mitigation/adaptation discussion at

Communicated by Juan Ignacio Lopez Moreno

✉ Piero Lionello
piero.lionello@unisalento.it

Luca Scarascia
luca.scarascia@le.infn.it

[1] DiSTeBA, University of Salento, Via per Monteroni 165, block M, Lecce, Italy

[2] CMCC, Euro-Mediterranean Center on Climate Change, Lecce, Italy

global scale. These two issues, considering specifically the north-south contrasts within the MedR, have not been addressed in the literature, though many papers analyzed future climate change in this region.

Changes of extreme precipitation, dry and of wet period length, are linked to the general concern of increasing intensity and frequency of droughts, on one hand, and of floods, on the other hand.

The Mediterranean region is among the regions that, since the mid-twentieth century, have been most exposed to hazards posed by droughts (Stagge et al. 2017; Caloiero et al. 2018; Spinoni et al. 2019). Suggestions of increasing dry conditions are provided by a majority of decreasing trend of total intense precipitation and of maximum duration of wet periods, on one hand, and of increasing duration of dry periods, on the other hand (e.g., Mathbout et al. 2018), though past changes of precipitation indices are not everywhere significant (e.g., Lionello et al. 2012. In fact, the reinforcement of drought events in this region is associated not only to lack of precipitation, but also to other thermodynamic processes, mostly related to increasing temperature, vapor pressure deficit, and land-surface feedbacks (e.g., García-Herrera et al. 2019; Miralles et al. 2019, Vicente-Serrano et al. 2014, Domínguez-Castro et al. 2019).

In the future, the Mediterranean drought events will become more severe, more frequent, and will last longer with relevant effects on processes that are related to the hydrological cycle (e.g., Lehner et al. 2017; Hertig and Tramblay 2017; Gosling et al. 2017; Pumo et al. 2016; Grillakis 2019; Koutroulis et al. 2018; Wanders et al. 2015). Future changes might be dramatic in the Mediterranean region, where droughts are projected to become much more frequent, even in moderate warming scenarios (Spinoni et al. 2018; Naumann et al. 2018). This will be associated with the future decline of total precipitation and increase of atmospheric evaporative demand (Vicente-Serrano et al. 2015; Vicente-Serrano et al 2019). Effects of droughts have been demonstrated to be important for ecosystems and economic sectors, such as agricultural production, affecting cereals, olives, tomatoes, wine grapes, and almonds (Kovats et al. 2014); for hydroelectric power production (García-Herrera et al. 2019), fires (Turco et al. 2017; García-Herrera et al. 2019), forests (Peñuelas et al. 2017), and vegetation (Gouveia et al. 2017).

River floods are a widespread problem in many Mediterranean countries. They produce the largest economic damage in northern countries, such as Italy, France, Greece, and Spain, but also in Turkey, and the largest number of victims in North African countries (mainly Algeria, Morocco, and Egypt, but also in Turkey and Italy, Llasat et al. 2010). In the period 1990–2006, total economic losses have been estimated—almost 30 billion Euros with more than 4500 victims (Llasat et al. 2010). Model projections suggest an intensification of precipitation extremes in some Mediterranean areas, with contrasting trends between northern and southern countries (e.g., Fowler et al 2007; Jacob et al. 2014; Scoccimarro et al. 2016; Tramblay and Somot 2018). Correspondingly, an increased flood risks, caused by increasing precipitation extremes, have been shown under a high emission scenario for north Mediterranean countries (Alfieri et al. 2015).

A large increase of temperature extremes and heat waves (intensity, number, and length) has occurred in the MedR in the last decades of the twentieth century (1960–2006) (e.g., Fischer & Schär 2010; Kuglitsch et al. 2010; Efthymiadis et al. 2011). Global and regional climate simulations agree on future increase of temperature extremes and heat waves across the whole Mediterranean region (Hertig et al. 2010; Jacob et al. 2014; Zittis et al. 2016).

An analysis of the impact of extreme temperatures under different climate change scenarios by 2100 concluded that Southern Europe will experience an increase of heat-related mortality and a decline of cold wave–related mortality (Gasparrini et al. 2017). In the Middle East and North Africa, heat-related mortality risk of elderly people by the end of the century under RCP8.5 could be 8–20 times higher compared with 1951–2005, and 3–7 times higher under RCP4.5 (Ahmadalipour et al. 2019). Considering a moderate population growth, attributable deaths per warm season in the north Mediterranean under RCP8.5 could increase by 20 and 59 thousand by mid- and end-century, respectively, while under RCP4.5, relevant figures would be 1.3 and 2.6 times lower, respectively (Kendrovski et al. 2017). Important for assessing different values of risks across the Mediterranean region is that the vulnerability of population to heat waves and temperature extremes is increased by poverty of population (Paz et al. 2016) and by aging (see Paravantis et al. 2017 for Athens and Greece and Paz et al. 2016 for Barcelona).

In the MedR, growing population is a problem in terms of food and water demand (Cramer et al. 2018). Evolution of population is unbalanced among different parts of the Mediterranean region. In Southern Europe (which includes all European countries along the Mediterranean coast and in the Balkans, but excludes France), population is predicted to decrease from 152 million in 2015 to 140 million in 2050. On the contrary, in the Middle East (Cyprus, Israel, Jordan, Lebanon, Syria, Palestine, and Turkey), it will increase from 126 to 173 million, and in North Africa (Algeria, Egypt, Libya, Morocco, Tunisia) from 186 to 279 million.[1] Beside different growth rates, situation is quite different also in terms of per capita gross national income (GNI). According to the United Nations[2], in 2012 all Europe countries (except Albania) were classified high income (more than 12.615 USD per capita

[1] Source: United Nations, Department of Economic and Social Affairs, Population Division (2017). World Population Prospects: The 2017 Revision, custom data acquired via website. https://population.un.org/wpp/DataQuery/

[2] Source: United Nations: https://www.un.org/en/development/desa/policy/wesp/wesp_current/2014wesp_country_classification.pdf

GNI), while the majority of the countries in the Middle East and North African areas were classified upper middle income (from 4085 to 12.615 USD per capita GNI). The exception are Israel (high income) and Syria, Morocco and Egypt (lower middle income, less than, but more than per capita GNI from 1035 to 4085 USD GNI). Therefore, demographic trends will pose higher demand of food, water, and energy from areas with presently lower economic resources in the MedR. This uneven socio-economic situation is an important motivation for estimating whether different regional climate change signal will be a driver that can further affect this imbalance.

In general analysis of precipitation extremes benefits from using regional climate models (RCMs), while simulated temperature extremes are less sensitive to model resolution. A discussion of GCM (global climate models) and RCM simulations in the MedR can be found in Planton et al. (2012). Past EU projects (PRUDENCE Christensen and Christensen 2007, ENSEMBLES, Déqué et al. 2012) have made available analyses of extremes in surface fields for the SRES scenarios (Nakićenović et al. 2000). Improved high resolution models are been successively developed and they have provided new results adopting the recent representative concentration pathways (RCP, Taylor et al. 2012), many of them within the MedCORDEX program (Ruti et al. 2015). However, this study aims at linking regional extremes to the global mean annual surface air temperature anomaly (GMASTA), and it needs a global temperature reference fields. This can be easily and directly accomplished analyzing GCM results. We admit that for precipitation extremes, this might reduce the size of the detected signal. However, a recent analysis shows that the climate change signal of precipitation extremes is not crucially depending on the model resolution, though the actual value of largest extremes (especially over steep orography) increases with resolution (Conte and Lionello 2019).

The novelty of this study is the analysis approach, which uses GMASTA as parameter to describe the evolution of regional extremes (as in Lionello and Scarascia 2018, but using difference indices) for providing information on their changes. Scholars and policymakers can use these outcomes in relation to the global temperature thresholds that are set in international agreements and negotiations. Further, this study is meant to provide a reference for contrasting trends of climate extremes at sub-regional scale.

The following "Data and methods" section describes the indices that are used to represent extremes in this study, the datasets and the methods to relate them to the GMASTA. "Results" section presents the results, separating them in three classes, i.e., maximum dry and wet spell duration, intense precipitation, frequency of cold days and warm nights. The paper is completed with "Discussion" section and "Summary and conclusions" section.

Data and methods

Definition of indices used in this study

This study considers 6 indices, selected among those recommended by the World Meteorological Organization (CCL/CLIVAR/JCOMM) and Expert Team on Climate Change Detection and Indices (ETCCDI) in the web page (http://www.clivar.org/organization/etccdi).

SDII (simple precipitation intensity index). Let RR_{wj} be the daily precipitation amount during the wet day w ($RR \geq 1$ mm) in year j. If N_W represents number of wet days in j, then $SDII_j = \sum_{w=1}^{N_W} RR_{wj}/N_W$.

R95pTOT, very wet day precipitation or annual total precipitation during very wet days. Let RR_{wj} be the daily precipitation amount in the wet day w in year j and let RR_{w95} be the 95th percentile of the RR_{wj} values in the 1961–1990 period. If N_W represents the number of wet days in the period, then $R95pTOT_j = \sum_{w=1}^{N_W} RR_{wj} where RR_{wj} > RR_{w95}$.

CDD (consecutive dry days), maximum length of dry spell, maximum number of consecutive days with $RR <$ 1 mm. Let RR_{ij} be the daily precipitation amount on day i in year j. CDD_j is the largest number of consecutive days in year j, where $RR_{ij} < 1$ mm.

CWD (consecutive wet days), maximum length of wet spell, maximum number of consecutive days with $RR \geq$ 1 mm. CWD_j is the largest number of consecutive days in year j, where $RR_{ij} \geq 1$ mm.

TN90p, percentage of days when TN > 90th percentile or percentage of warm nights. Let TN_{ij} be the daily minimum temperature on day i in year j and let TN_{n90} be the calendar day 90th percentile centered on a 5-day window for the base period 1961–1990. $TN90p_j$ is the percentage of days in the year j when $TN_{ij} > TN_{n90}$, that is nights are warmer than in the base period.

TX10p, percentage of days when TX < 10th percentile or percentage of cold days. Let TX_{ij} be the daily maximum temperature on day i in period j and let TX_{n10} be the calendar day 10th percentile centered on a 5-day window for the base period 1961–1990. $TX10p_j$ is the percentage of days when $TX_{ij} < TX_{n10}$, that is days are colder than in the base period.

Data used

The 6 indices have been extracted from http://www.cccma.ec.gc.ca/data/climdex/climdex.shtml. This archive allows to download the indices computed by Sillmann et al. 2013a and b.

The results of 28 CMIP5 (Coupled Model Intercomparison Project Phase 5) models (see table 1 in Lionello and Scarascia 2018, with the list of models and their mean characteristics) have been used. These models have a median grid with 180 longitudes, 96 latitudes, and 39 vertical levels. The data used in this study covered the period 1901–2100 and the RCP8.5 scenario.

Here, three reanalysis datasets are used, namely, the NCEP reanalysis (National Centers for Environmental Prediction/National Center for Atmospheric Research, Kalnay et al. 1996, Kistler et al. 2001) and two ECMWF (European Center for Medium-Range Weather Forecasts) reanalysis products, ERA40 (Uppala et al. 2005) and ERA-Interim (Dee et al. 2011). The indices extracted from these three datasets cover different periods, specifically 1948–2010, 1958–2001, and 1979–2010, in this order. Reanalyses are used to validate the values of the extreme indices computed by the climate models during the 1971–2000 period (see "Discussion" section).

The analysis considers the Mediterranean region (MedR from 30 N to 46 N and from 7 W to 37 E), which coincides with the selection adopted in Lionello and Scarascia (2018). It is further split in north Mediterranean (NMed) and south Mediterranean (SMed) using 38 N as dividing latitude.

Methods

The same methods described in Lionello and Scarascia (2018), where a more detailed explanation is available, have been used.

Annual/seasonal average anomalies of indices are associated to the corresponding GMASTA anomaly and grouped in 1 K wide bins, centered around GMASTA values from − 1 to + 4 with respect to the 1971–2000 mean value. For each bin and each model, the average value of the indices is computed. The ensemble model mean is used to describe the evolution of indices as GMASTA increases (Figs. 1 and 2).

Further, the rate of change r of the indices with changes of GMASTA is estimated, both locally and aggregating data for the NMed and SMed regions. The rate is given by the Theil-Sen estimate (Theil 1950; Sen 1960) that is the median of the values $r_{ij} = (I_i - I_j)/(\mathrm{GMASTA}_i - \mathrm{GMASTA}_j)$, where I_i and GMASTA_i are the values of the index I and of GMASTA in the same year i. The value of r is estimated for each GCM, for the NMed and the SMed areas, and at every point of a common 1 × 1.25 (lat × lon) grid. This procedure provides information on geographical variation of trends, producing a set of best estimates of dI/dGMASTA, rate of change of the index I with global warming. The median of the 28 dI/dGMASTA, with the uncertainty given by the 5th and 95th percentiles as uncertainty range, is the outcome of the procedure. Figure 3 shows the results aggregated on the NMed and SMed, and Fig. 4 shows the spatial distribution of rates of change.

In the case of TN90 and TX10, a preliminary analysis (see Figs. 1 and 2, panels **e** and **f**) shows that a linear rate of change would be a poor reproduction of the variation of these two indices with GMASTA. For these two indices, seasonal values corresponding to the 2 K and 4 K GMASTA thresholds are computed and used in maps and statistics (Figs. 5 and 6).

Results

Maximum dry and wet spell duration

Figure 1 a and b show the evolution of the CDD and CWD anomalies (units, days) with respect to the 1971–2000 mean values of the indices for the NMed and SMed, respectively. As global warming increases, dry spells will become longer and wet spells become shorter than now, both in the NMed and

Table 1 Rate of change of extreme indices (CDD, CWD, SDII, R950TOT) as GMASTA increases. Columns report the minimum; the 10th, 50th, and 90th percentiles; maximum of the model ensemble; and the trend of the ensemble mean for the NMed (columns 2–8) and the SMed (columns 9–14). Lines denoted using ENS20 and ENS21 consider separately the values computed using data of the twentieth and twenty-first century. The values that are statistically significant considering model uncertainties are marked with italic and larger characters

		NMed						SMed					
		Min.	10th p	50th p	90th p	Max	Mean	Min.	10th p	50th p	90th p	Max	Max mean
CDD (days/K)	ENS20	− 7.1	− 5.3	1.2	4.6	8.3	2.4	− 21.4	− 11.4	2.7	16.2	29.2	8.2
	ENS21	0.7	2.0	*5.0*	7.5	9.6	5.0	2.2	3.4	*7.3*	15.6	22.4	9.6
CWD (days/K)	ENS20	− 2.0	− 1.5	− 0.3	0.1	0.3	− 0.6	− 1.2	− 0.9	*− 0.4*	0.0	0.5	− 0.5
	ENS21	− 1.0	− 0.8	*− 0.5*	− 0.2	− 0.2	− 0.5	− 1.0	− 0.9	*− 0.5*	− 0.2	− 0.2	− 0.3
SDII (mm/K)	ENS20	− 0.17	− 0.07	0.08	0.28	0.37	− 0.03	− 0.27	− 0.18	0.00	0.35	0.72	− 0.08
	ENS21	− 0.09	0.02	*0.09*	0.18	0.24	0.10	− 0.15	− 0.06	0.01	0.09	0.12	0.02
R95pTOT (mm/K)	ENS20	− 23.6	− 6.2	9.5	23.7	46.8	5.1	− 14.3	− 9.5	− 2.6	9.3	17.0	− 4.0
	ENS21	− 8.9	− 2.2	5.3	10.1	11.4	4.0	− 5.6	− 3.8	− 1.9	1.2	2.6	− 1.4

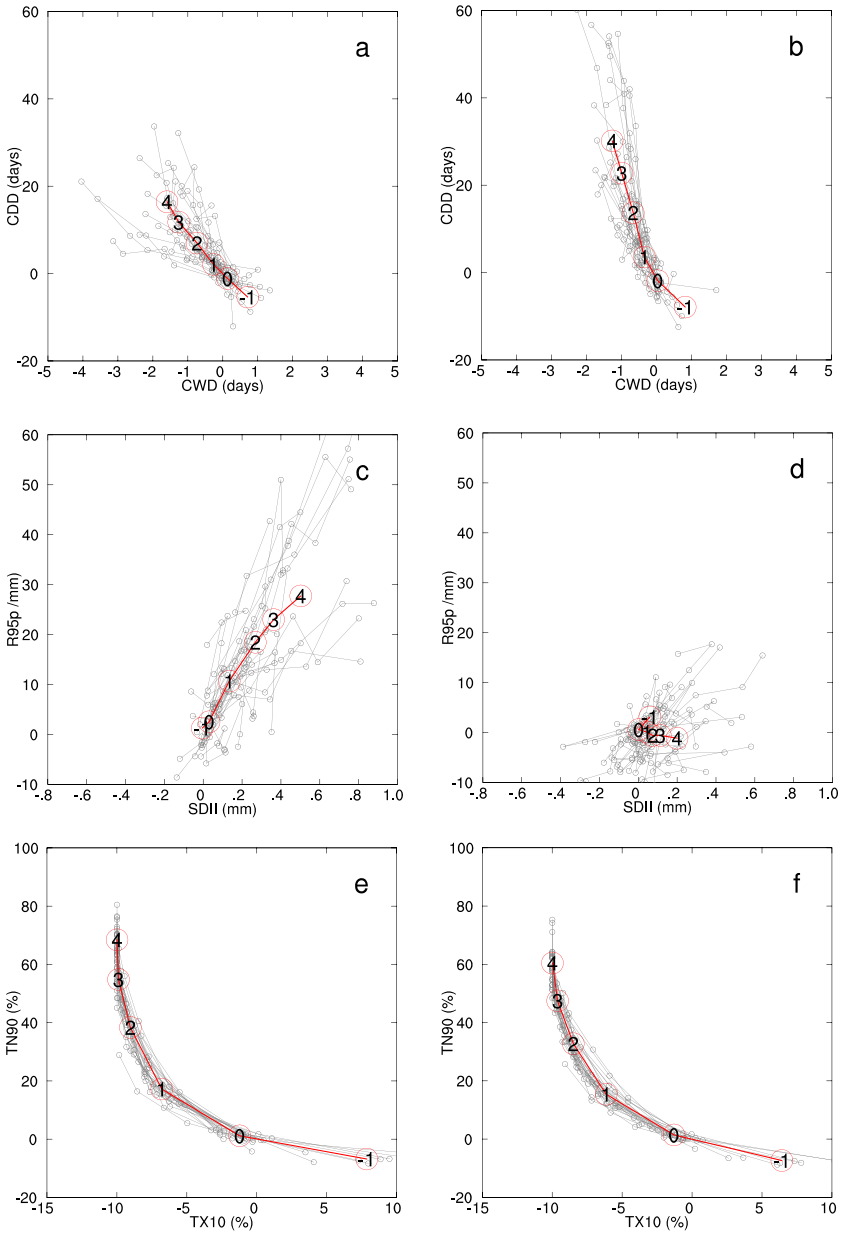

Fig. 1 Evolution of climate extremes in the Mediterranean region with global warming. Climate indices are shown for the north (left column) and south (right column) Mediterranean region as a function of global mean annual surface temperature anomaly (GMASTA) with respect to the 1971–2000 period. Gray lines are individual models. The red thick line is the model ensemble mean (values inside circles represent the GMASTA along the ensemble mean trajectory). Top row (**a**) and (**b**), maximum dry (CDD) versus maximum wet spell (CWD) duration. Mid row (**c**) and (**d**), annual total precipitation in days exceeding the 95th percentile threshold (R95pTOT) versus mean daily precipitation amount of wet days (SDII). Bottom row (**e**) and (**f**), percentage of days with minimum temperature above the 90th percentile threshold (warm nights, TN90p) versus percentage of days with maximum temperature below the 10th percentile threshold (cold days, TX10p). Values of indices represent anomalies with respect to the 1971–2000 reference mean

SMed. However, the reduction of wet spell maximum duration is appreciably larger in the NMed than in the SMed, while increase of dry spell is smaller in the former than in the latter. The behavior is almost linear with global warming, and there is a strong consensus among models.

Figure 2a considers the actual values of CDD and CWD and evidences the climate differences between NMed and SMed. In the present climate condition in the NMed, dry and wet spell have maximum durations in the order of 40 and 12 days, respectively. In the SMed, the maximum duration of dry spells exceeds 100 days (mostly because of a strong influence of the arid areas in North Africa) and is much longer than in the NMed. On the contrary, in the SMed, maximum duration of wet spell is much shorter (it is approximately 7 days) than in the NMed. Percent-wise, the effect of climate change on these two indices is similar in the NMed and SMed, but it will, in fact, increase the climate contrast between the two areas.

Figure 2a reports also the mean values of CDD and CWD in the NCEP, ERA-40. and ERA-Interim reanalysis in the period 1961–1990, which are meant to be compared with the ensemble mean values corresponding to a small, practically nil, GMASTA anomaly. Differences among these reanalyses are particularly large for CWD in the NMed. Climate models underestimate CDD with respect to reanalyses in the SMed, while there is a substantial agreement in the NMed.

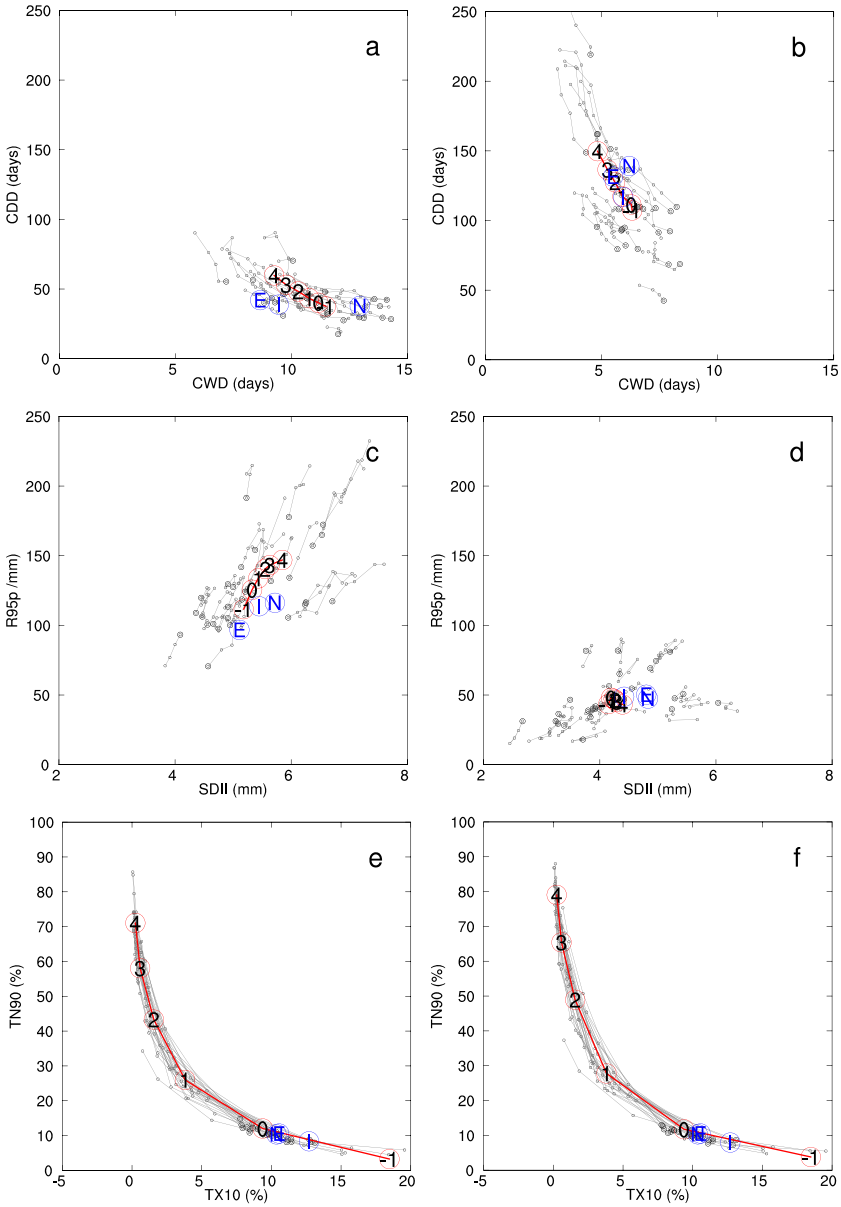

Fig. 2 Same as Fig. 1, except the actual values of the indices values are shown. The blue circles, with labels N, E, I, show the reanalyses NCEP, ERA40, ERA-Interim, respectively, for the period 1971–2000 (1979–2000 for ERA-Interim). The labels N and E overlap in panels **d**, **e**, and **f**

Figure 3 (as well as Table 1) shows the values of the rate of change of CDD and CWD with GMASTA in SMed and NMed, separately for the twentieth and twenty-first century. It reports the 10th, 50th, 90th, the mean, and the maximum and minimum among models. The intermodal spread is very large and prevents the detection of any significant relation with GMASTA during the twentieth century, when only the decrease of CWD in the SMed is marginally significant. However, during the twenty-first century, as GMASTA increases, the rate of change of both indices becomes significant in both SMed and NMed. For the twenty-first century, the rate of change of CDD is 5.0 days/K (1.9; 7.6)[3] for the NMed and 7.3 days/K (3.2; 15.9) for the SMed, the rate of change of CWD is − 0.5 days/K (− 0.8; − 0.2) for the NMed and − 0.3 days/K (− 0.5; − 0.2) for the NMed.

Figure 4 shows more details on the spatial variability of the rate of change of CDD and CWD as GMASTA increases. The decrease of CWD (Fig. 3a) is largest in the central latitudinal band of the Mediterranean (with maxima over Northwestern Iberia, where it is stronger than − 0.8 days/K, the Balkan and Anatolia peninsula) and it becomes weaker than − 0.4 days/K along the northern and southern boundaries of the MedR. The rate of change of CDD increases southwards, with values increasing from a minimum of 3 days/K at the northernmost coast of the Mediterranean Sea to 12 days/K along its North African coastline.

These results suggest that in the MedR, droughts will become more severe (longer) in the future than in the present,

[3] Among brackets, the 10th to 90th percentile range is reported.

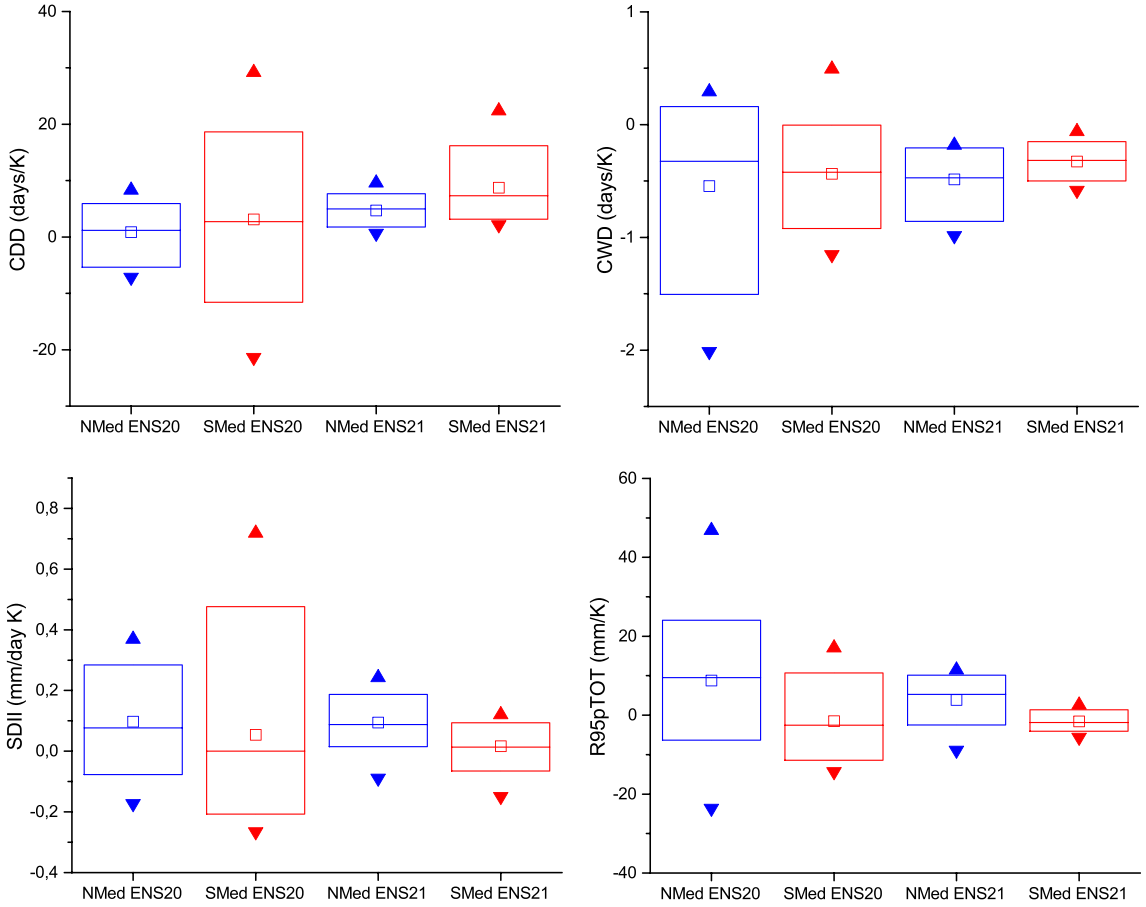

Fig. 3 Rate of change of hydrological extremes during the twentieth and twenty-first century. Panels represent the rate of change of CDD (top-left), CDW (top-right), SDII (bottom-left), R95pTOT (bottom-right) as a function of GMASTA. Label along the *x*-axis of the panels denote the twentieth (ENS20) and twenty-first (ENS21) century and the NMed (blue colors) and SMed (red colors). The lower and upper boundary of the boxes show the 10th and 90th percentiles, the inner line is the 50th percentile, squares show the ensemble mean, triangles denote maximum and minimum values among models.

while prolonged period of persistent precipitation will become shorter. However, this effect will be unbalanced between NMed and SMed, with the increase of extreme dry spell length affecting more the SMed than the NMed and the reduction of extreme wet spell length affecting more the NMed than the SMed.

Intense precipitation

Figure 1 c and d show that the link of global warming to intense precipitation is quite different in NMed (where intensity of precipitation increases) and SMed (where changes are small). In the NMed, both SDII (mean daily precipitation during wet days) and R95pTOT (average annual total precipitation in days exceeding the 95th percentile intensity threshold) increase substantially with global warming. In the SMed, R95pTOT does not change, and SDII increase is of marginal relevance.

If instead of anomalies, the actual values of the two indices are considered (Fig. 2 c and d), the climate differences between NMed and SMed are evident for intense precipitation, with both R95pTOT and SDII having larger values in the NMed than in the SMed. It other terms, the precipitation regime is already presently more intense in the NMed than in SMed, and global warming will further increase this difference. However, the presence of two model families producing two different evolution of SDII and R95pTot is suggested by Figs. 1c and 2c. This confirms that individual climate models present relevant differences in their estimates of intense precipitation events.

Figure 2b reports also the mean values in the 1961–1990 period of SDII and R95pTOT in the NCEP, ERA-40, and ERA-Interim reanalysis. The agreement on the value of SDII among the reanalyses and between reanalyses and models is debatable. The most robust indication is that climate models underestimate SDII in the SMed. The value of RCP965 is less controversial.

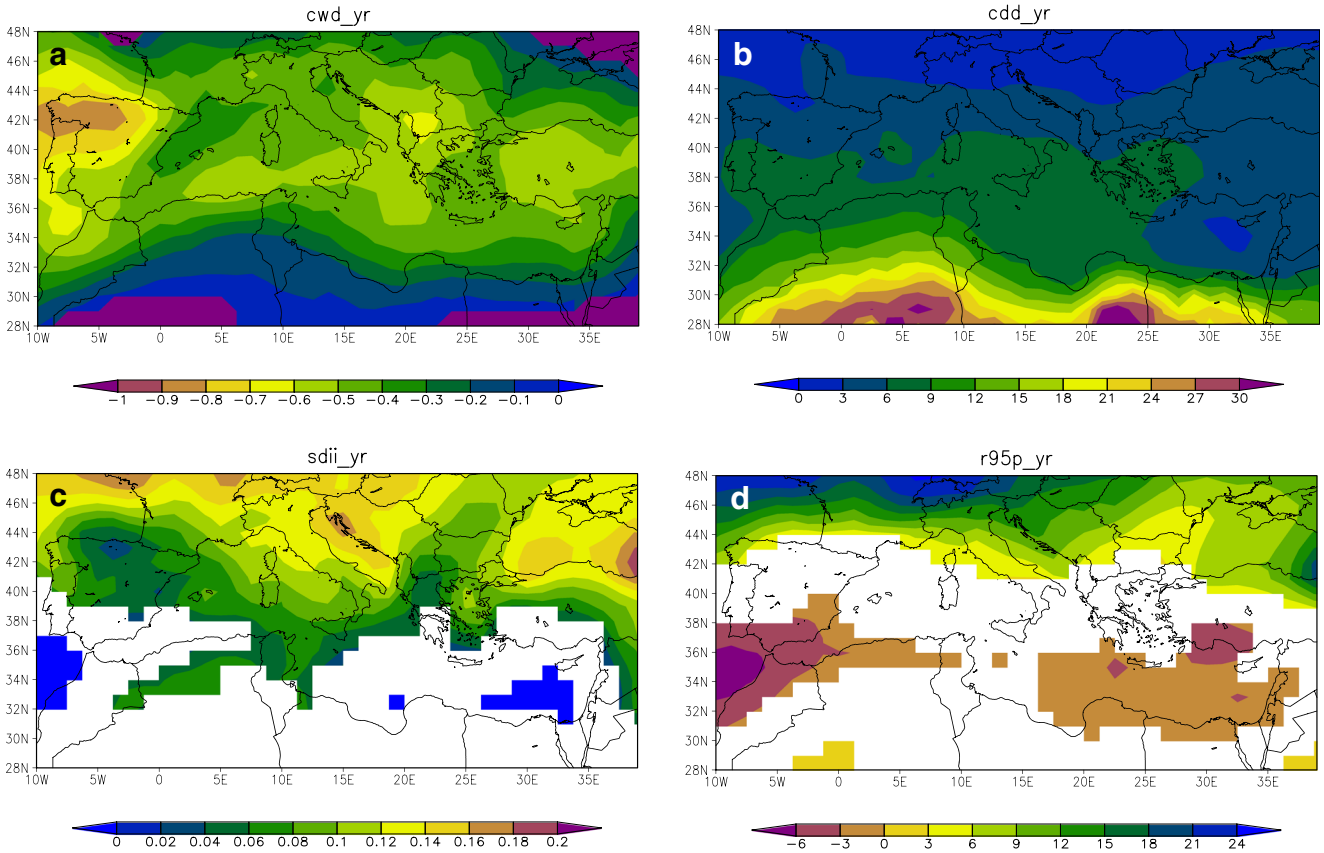

Fig. 4 Spatial distribution of the rate of change with global temperature of hydrological extreme indices. **a** Maximum wet spell length (CWD; units, days/K). **b** Maximum dry spell length (CDD; units, days/K). **c** Simple precipitation intensity index (SDII; units, mm/K). **d** Annual total precipitation during intense rain day events (R95pTOT, daily rain total in days with precipitation above the 95th percentile; units, mm/k)

Figure 3 (as well as Table 1) shows the rate of change of SDII and R95pTOT in the SMed and NMed, separately, for the twentieth and twenty-first century. The intermodal spread of SDII and R95pTOT is larger than that of CDD and CWD. In general, the 10th to 90th percentile uncertainty range does not allow detecting the presence of a statistically significant link of those two indices with global warming, except for the (marginal) increase of SDII in the NMed. This indicates that

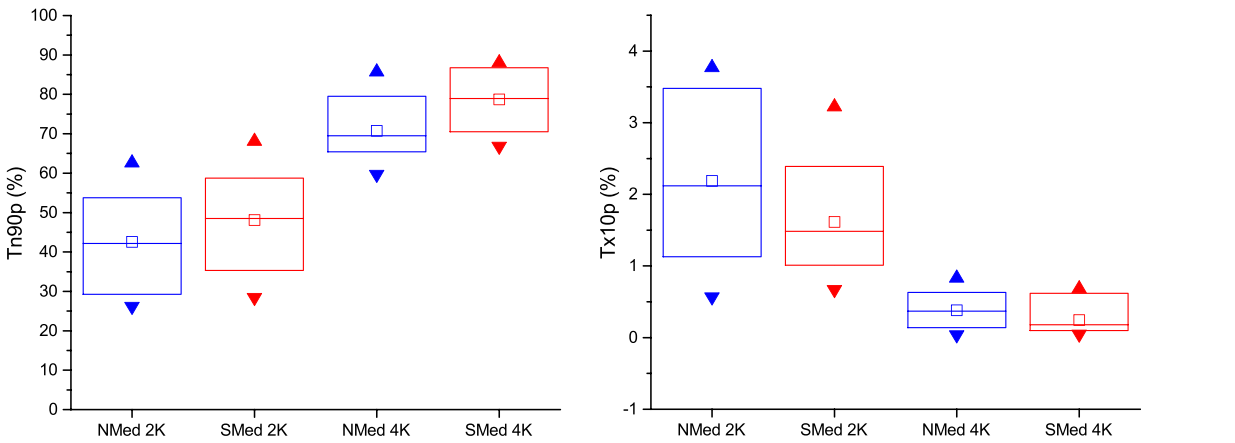

Fig. 5 Cold day and warm night frequencies as global warming increases. The two panels show the values of Tn90p (left) and Tx10p (right) when GMASTA reaches the 2 K and 4 K thresholds for the NMed (blue) and SMed (red). The lower and upper boundary of the boxes show the 10th and 90th percentiles, the inner line is the 50th percentile, squares show the ensemble mean, triangles denote maximum and minimum values among models

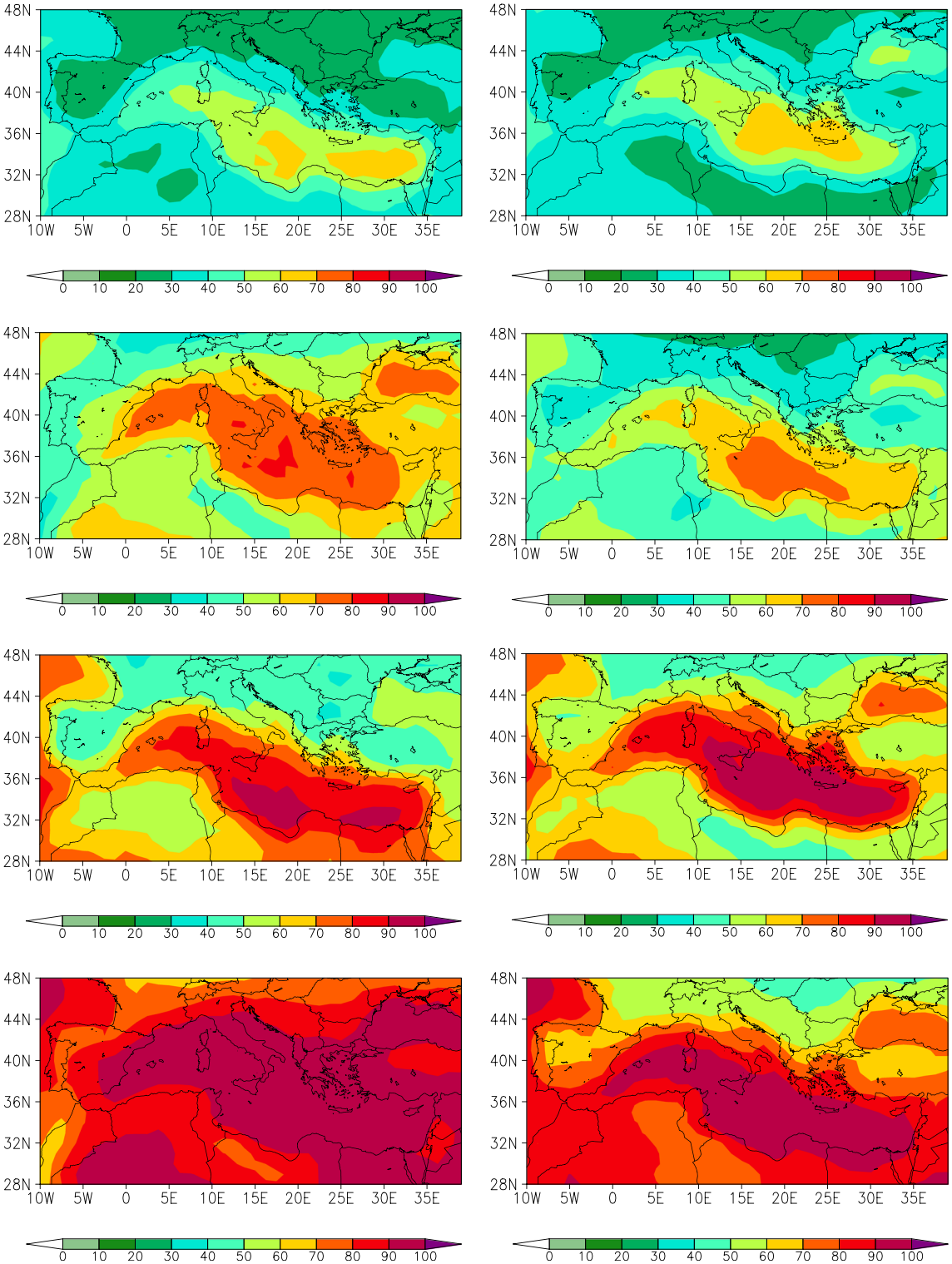

Fig. 6 Spatial distribution of the frequency (%) of warm nights when the global mean surface temperature anomaly reaches the 2 K and 4 K thresholds. Each panel refers to the different seasons. Winter (DJF, Dec-Jan-Feb), spring (MAM, Mar-Apr-May), summer (JJA, Jun-Jul-Aug), autumn (SON, Sep-Oct-Nov). All values are statistically significantly different with respect to the 10% reference value. Labels on top-left corner of each panel denote the field

internal variability and model-related uncertainty prevents reaching statistically significant conclusions for those two indices. However, the ensemble mean values of the rate of change of both indices are positive and large during the

Table 2 Average fraction (%) of cold days (TX10) and warm nights (TN90). Different lines report values for 2 K and 4 K GMASTA anomalies. Columns show the minimum; the 10th, 50th, and 90th percentiles; maximum of the model ensemble; and the trend of the ensemble mean for the NMed (columns 2–8) and the SMed (columns 9–14). The values that are statistically significant considering model uncertainties are marked with italic and larger characters

		NMed						SMed					
		Min.	10th p	50th p	90th p	Max	Mean	Min.	10th p	50th p	90th p	Max	Mean
TX10 (%)	2 K	0.6	1.4	*2.2*	3.3	3.8	2.2	0.7	1.1	*1.6*	2.3	3.2	1.6
	4 K	0.0	0.2	*0.4*	0.6	0.8	0.4	0.1	0.1	*0.2*	0.5	0.7	0.2
TN90 (%)	2 K	26	32	*42*	52	63	43	28	36	*48*	58	68	48
	4 K	60	65	*69*	78	86	71	67	72	*78*	86	88	79

twenty-first century in the NMed, where the rate of change of SDII is 0.1 mm/K (0.0; 0.2)[4] and of R95pTOT is 5.3 mm/K (−2.0; 10.1).

Figure 4 shows that the uncertainty of the overall rate of change of intense precipitation in the NMED and SMED is partially caused by large spatial variability within the areas. Considering SDII, all significant rate of change are positive. While in the SMED, few significant values are present, most of the NMed is covered with positive values, reaching 0.15 mm/day at the northern border of the area. Considering R95pTot, its rate of change with GMASTA is not significant over large areas of the MedR. However, there is small significant decrease (around 3 mm/K) in some area of the SMed and a substantial increase along the northern boundary of the MedR (reaching values close to 20 mm/K). Therefore, aggregating data over the whole NMed and SMed hides changes that are significant over large areas and suggests (i) for R95pTot, contrasting terms between NMed (positive) and SMed (negative); (ii) for SDII, a significant increase over large areas of the NMed.

These results show that the evolution of intense precipitation with global warming will further increase the differences between the NMed (already characterized with intense events) and the south (where events are comparatively milder). Both the average intensity of rain (represented with SDII) and the fraction of rain occurring during intense events (R95pTOT) will increase with global warming over large areas of the NMed, while changes will be small or negligible in the SMed.

Cold nights and warm days

At difference with the response of the regional precipitation regimes to global warming, frequencies of warm nights (TN90p) and cold days (TX10p) as a function of global warming are similar in the NMed and SMed (Figs. 1e–f and 2e–f; Table 2).

The evolution of these two indices with GMASTA in Figs. 1e–f and 2e–f cannot be realistically represented by a linear behavior. Therefore, at difference with respect to "Maximum dry and wet spell duration" and "Intense precipitation" sections, instead of discussing their rate of change as GMASTA increases, Fig. 5 shows their values when GMASTA reaches the 2 K and 4 K thresholds. In both areas, the increase of warm nights is dramatic, to the extent that 69% (65%, 78%) and 78% (72%, 86%) of them would be classified as warm nights[5] in the NMed and SMed, respectively, for a 4 K increase of GMASTA (Fig. 5 and Table 2). The percentages will be smaller (42% [32%, 52%] and 48% [36%, 58%], respectively), but anyway very relevant for a 2 K increase of GMASTA.

Considering cold days (Fig. 5 and Table 2), both in the NMed and SMed for a 4 K increase of GMASTA, there will be almost no cold days, and for a 2 K GMASTA their frequency will be reduced to about 2%. The consensus among models in Figs. 1e–f, 2e–f, 5, Tables 1 and 2 is impressive.

The agreement on values of these temperature extremes between climate models and reanalyses is acceptable. In fact, the values of TN90p and TX10p based on the NCEP, ERA-40, and ERA-Interim reanalyses are located along the lowest part of the climate model trajectories in correspondence to a small negative GMASTA.

Figure 6 shows the spatial distribution of the frequency of warm nights when GMASTA reaches the 2 K and 4 K threshold. The percent increase of warm days is larger in summer than in winter. This is consistent with Lionello and Scarascia (2018), who have shown that the increase of minimum daily temperature is larger in summer than in winter. Further, the increase of TN90p is larger above sea than above land. Similarly, the decrease of cold days (Fig. 7) will be also larger in summer than in winter and larger over sea than over land. Charges are dramatic. For a 4 K temperature increase, in summer, everywhere over sea, almost all nights would be classified warm, and there will be no cold days anywhere in

[4] Among brackets, the 10th to 90th percentile range is reported.

[5] Here, the definition of warm nights and cold days is based on the 1961–1990 reference period

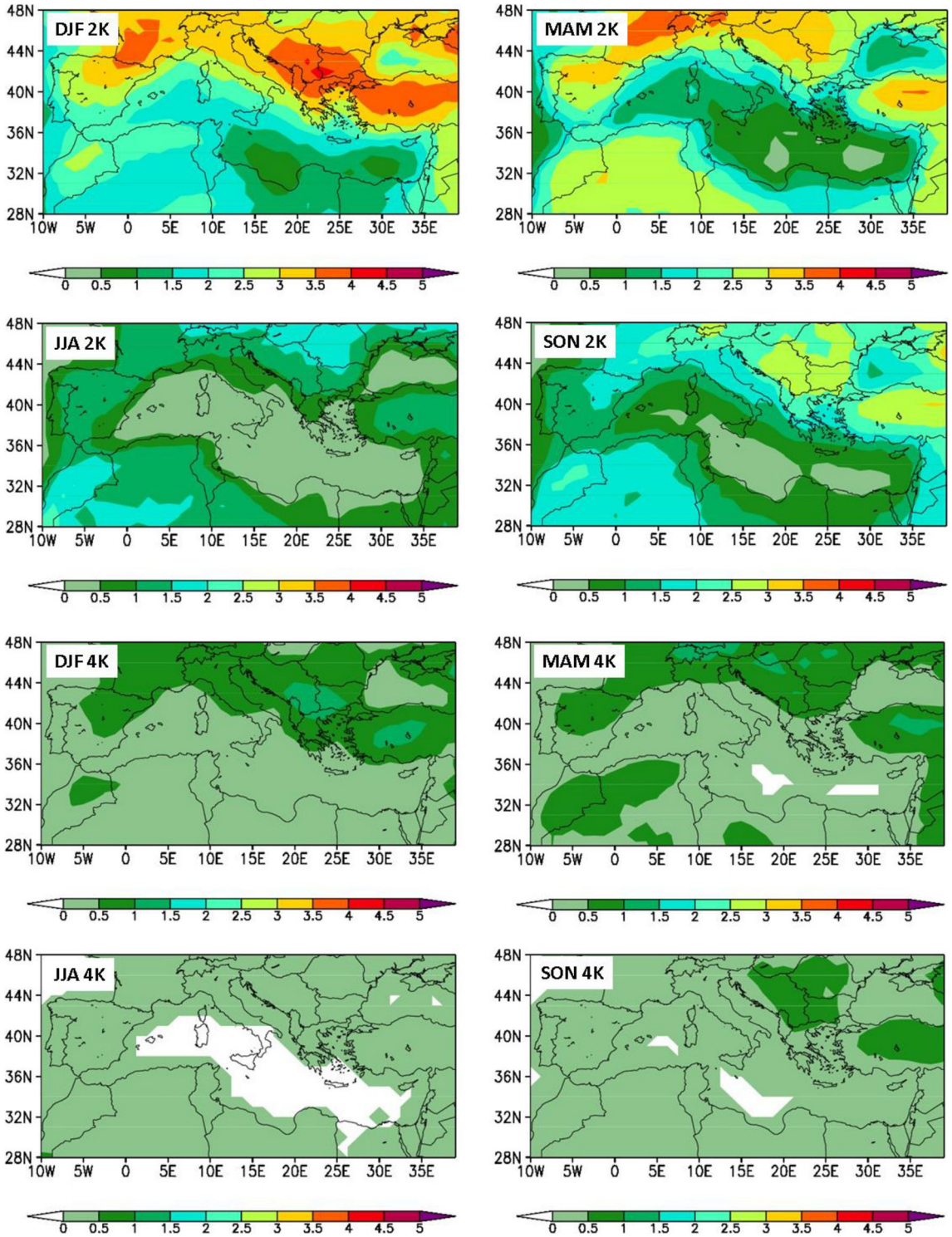

Fig. 7 Same as Fig. 6, except it refers to the frequency of cold days

the MedR. Among the considered season and the two GMASTA thresholds, changes are smallest in winter for the 2 K GMASTA increase. However, also in such case changes will be large, particularly in several areas of the SMed. Obviously, definitions of warm nights and cold days refer to the 1971–2000 reference period.

Discussion

The future evolution of climate extremes has been described in several former studies, which have already shown their strong sensitivity to climate change in the MedR. On this respect, this study is consistent with former results, but it

focuses on the distinction between NMed and SMed and the dependence on global temperature changes. The Mediterranean region as a whole is mentioned in Sillmann et al. (2013b) for increase of duration of dry periods, temperature maxima (particularly in summer), frequency of warm and tropical nights, and decrease of heavy precipitation. Other authors, often at subregional scale or for specific countries, have further investigated the results of Sillmann et al. (2013b). The future increase of heat extremes has been confirmed for southern Europe (Beniston et al. 2007), North Africa, and the Middle East (Lelieveld et al. 2016; Zittis et al. 2016). The future evolution of precipitation and dry period extremes has been analyzed in several studies, often at sub-regional and country scale (e.g., for Italy by Zollo et al. 2016 and for Israel by Hochman et al. 2018), but also at regional and larger scale (e.g., Scoccimarro et al. 2016; Tramblay and Somot 2018; Samuels et al. 2018), which emphasized the increase of precipitation extremes in some areas. With respect to these former studies, our study shows that the geographical differences within the MedR can be described in terms of a strong north-south contrast that increases with global warming.

Reliability of GCMs in reproducing values of extreme indices is an important issue, but it is clearly beyond the scope of this paper and it would require a different investigation for each variable. In fact, mechanisms leading to model errors or responsible for uncertainties are specific of each considered index. However, Fig. 2 reports also the reference values for the period 1961–1990 in the NCEP, ERA-40, and ERA-Interim reanalyses, which can be approximately compared with the ensemble mean value corresponding to a nil GMASTA anomaly.

Figure 2 shows that the uncertainty on the reference values (qualitatively represented by the differences among the reanalyses) is, in most cases, comparable with their discrepancies with respect to the model ensemble mean for a nil GMASTA change. In other words, for most indices, the error of the ensemble mean is comparable with the uncertainty of the real reference value. Climate models are not accurate only for CDD in the SMed and R95pTOT in the NMed (they clearly underestimate and overestimate, respectively, the values of these two indices the reanalyses). Therefore, apart these two exceptions, the comparison with reanalyses support the capability of the ensemble mean to reproduce the mean past values of the considered indices and their differences between NMed and SMed.

In few cases, the variations of some variables associated with a GMASTA change from − 1 to + 4 are actually comparable with their differences with respect to the reanalyses. In this case, it is difficult to separate model uncertainties from climate change estimates. This happens for CWD and SDII in the NMed, and R95pTOT and SDII in the SMed.

Considering the indices describing the extremes of the hydrological cycle (CDD and CDW, Figs. 2 a and b), there are interesting differences between NMed and SMed. The variation with climate change of CWD is smaller than the differences among reanalyses. In other words, uncertainty on the present value of CWD is larger than their change with climate change produced (actually with a remarkable consistency among themselves) by models. Instead, in the NMed, the value of CDD appears consistent among the three reanalyses and the model ensemble mean. Therefore in the NMed, the confidence on the increase of CDD with global warming appears stronger than that on the reduction of CWD. Considering extreme precipitation events in the NMed, the uncertainty in SDII provided by reanalyses is large, and R95pTOT is systematically overestimated by models. SDII is underestimated in SMed, where, anyway, no trend is suggested by climate models. Both in the NMed and SMed, it appears that models overestimate the number of warm night and underestimate the number of cold days.

Further issues are the consensus among models and whether the ensemble mean represents adequately their behavior, or there are relevant outliers. Figure 1 shows that different models exhibit a remarkable consensus on changes of extreme indices with GMASTA. This is true for both the direction and the magnitude of the changes, suggesting a robust common background driving them. In general, models agree more on changes of the indices (Fig. 1) than on their actual values (Fig. 2). Their consensus on extreme temperature indices (TN90 and TX10) is remarkably larger than on precipitation indices (R95pTOT and SDII). Figure 2 shows that models disagree substantially on the actual values of SDII and R95pTOT but, in spite of this, agree on their variations with climate change in the NMed, where both indices increase with global warming in all models (Fig. 1). Figure 1e shows that the ensemble mean results from averaging two distinct sets of model that agree on the increase of R95pTOT in NMed, but differ by a factor 2 in its magnitude. In this case, there is no uncertainty on the future increase of the index, but the ensemble mean is not likely to represent the actual future evolution.

Summary and conclusions

Length of dry and wet periods

As global temperature rises, a strong general tendency towards longer dry period and shorter wet spells will affect the whole Mediterranean region, but with important differences between north and south areas.

The maximum duration of dry spell is already longer in the SMed than in the NMed. Table 3 shows the reference values in the NCEP, ERA40, ERA-Interim reanalyses, which, depending on the dataset, vary in the range (117–139 days) in the

Table 3 Averages of the extreme value indexes in the NCEP, ERA-Interim, and ERA-40 reanalyses. Averages are computed considering all years when the corresponding GMASTA is inside a 1 K wide bin centered on the mean value of the 1971–1990 period

	NMed			SMed		
	NCEP	ERA-Interim	ERA-40	NCEP	ERA-Interim	ERA-40
CWD (days)	38	39	42	139	117	132
SDII (mm/day)	13	9.5	8.5	6.2	5.9	5.5
R95pTOT (mm)	5.7	5.4	5.1	4.8	4.4	4.8
TX10 (%)	116	114	97	47	49	50
TN90 (%)	10.4	8.2	10.6	10.4	8.2	10.6
CDD (days)	10.4	12.2	10.6	10.3	12.8	10.5

SMed and (38–42 days) in the NMed. The effect of climate change will increase such length of 7.3 days and 5.0 days per degree of global warming in the NMed and SMed, respectively.

The maximum duration of wet spells is larger in the NMed than in the SMed. Table 3 shows the reference values in the NCEP, ERA40, ERA-Interim reanalyses, which, depending on the dataset, vary in the range (5.5–6.2 days) in the SMed and (8.5–13 days) in the NMed. The effect of climate change will be similar in the two areas, reducing it to 0.5 days per degree of global warming. In the SMed, this trend is significant already during the twentieth century.

Therefore, the increase of dry period maximum length will be substantially larger for the SMed than for the NMed, further increasing the differences in hydrological extremes between these two areas, while the maximum length of wet spells will decrease at a similar rate in both areas.

Intense precipitation events

Climate change will also increase the differences between intense precipitation events in the NMed and SMed. Our analysis was not able to consider extreme precipitation events, but two indicators of their average intensity, i.e., the average precipitation during rainy days (SDII) and the total precipitation during intense precipitation events (R95pTOT).

The reference value of SDII in the NMed is in the range of 5.1–5.7 mm and in the SMed in the range of 4.4–4.8 mm. Trends with global temperature increase are positive and larger in the NMed, where a significant increase of 0.09 mm/K per degree of global warming is expected during the twenty-first century. Particularly large and significant values are over land along the northern boundary of the MR (Alps) and the eastern boundary of the Adriatic Sea. No clear variation with global warming of SDII is found in the SMed.

The contribution of intense events to the precipitation total is twice as large in the NMed as that in the SMed. The reference value of R95pTOT in the NMed is in the range of 97–116 mm and in the SMed in the range of 47–50 mm. Rates of change with GMASTA are positive in the NMed and negative in the SMed, but not statistically significant when the two entire sub-regions are considered. However, maps shows that locally future trends are statistically significant and negative along large parts of the North African and Middle East coasts, statistically significant and positive along the northern boundary of the Mediterranean region.

Warm nights and cold days

Changes of temperature extremes are to a large extent homogeneous in the NMed and SMed. For the considered indicators, changes are already significant in the twentieth century and potentially dramatic in the future. With a 2 K global warming, cold days will be rare both in the NMed (2.2%) and SMed (1.6%) and practically disappear with a 4 K temperature increase (0.4% in the NMed and 0.2% in the SMed). At the same time, warm nights will become common with a 2 K global warming (42% in the NMed and 48% in the SMed) and the majority with a 4 K global warming (69% in the NMed and 78% in the SMed). The actual values suggest that the effect of climate change on temperature extremes will be marginally larger in the SMed than in the NMed, but differences between the two areas are not statistically significant.

Seasonal and regional characterization of trends of temperature extremes is substantial. Summer will be much more affected than winter and changes will be smaller in the NMed continental areas than in the rest of the MR. In the central areas of the MR in summer, three out of four nights for a 2 K global temperature increase, and all nights for a 4 K increase will be warm. Over the same areas, cold days will practically already disappear with a 2 K GMASTA increase.

An increasing north-south contrast

These results emphasize the critical issues related to subregional aspects of global warming and the importance of

limiting it. This study presents a clear indication that as global warming increases, the differences of hydrological cycle and intense precipitation between north and south Mediterranean areas that already exist will become larger. The dependence with respect to GMASTA shows that impacts are already evident with a 1 K global warming with respect to the 1971–2000 average and differences between a 2 K and a 4 K increase are quantitatively important.

Different climate change signals overlap with large differences in wealth and population dynamics. Even changes of temperature extremes, which are to some extent homogeneous, when superimposed with such background differences, will likely lead to quite different risk levels between north and south Mediterranean areas. We stress that particularly future changes of the hydrological cycle have the potential of further increase critical socio-economic north-south contrasts, as they look to further increase water scarcity problems that already exist where socio-economic situation is less favorable.

Abbreviations CDD, annual maximum length of consecutive dry days; units, number of days; CMIP5, Coupled Model Intercomparison Project Phase 5; CWD, annual maximum length of consecutive wet days; units, number of days; GCM, global climate model; GMASTA, global mean annual surface air temperature anomaly; GNI, per capita gross national income; MedR, Mediterranean region (from 30 N to 46 N and from 7 W to 37 E); NMed, north Mediterranean areas (areas of MedR north of 38 N); SDII, standard daily intensity index (mean daily precipitation during wet days; units, millimeter); SMed, south Mediterranean areas (areas of MedR south of 38 N); SRES, special report on emission scenarios; R95pTOT, average annual total precipitation in days exceeding the 95th percentile intensity threshold (units, millimeter); RCM, regional climate model; RCP, representative concentration pathway; TN90p, percent of warm nights, fraction (%) of days with minimum temperature above the 90th percentile of the daily minimum temperature of the 1961–1990 period; TX10p, percent of cold days, fraction (%) of days with maximum temperature below the 10th percentile of the daily maximum temperature of the 1961–1990 period

References

Ahmadalipour A, Moradkhani H and Kumar M (2019) Mortality risk from heat stress expected to hit poorest nations the hardest. Climatic Change 152:569–579. https://doi.org/10.1007/s10584-018-2348-2

Alfieri L, Feyen L, Dottori F, Bianchi A (2015) Ensemble flood risk assessment in Europe under high end climate scenarios. Glob Environ Chang 35:199–212. https://doi.org/10.1016/j.gloenvcha.2015.09.004

Beniston M, Stephenson DB, Christensen OB, Ferro CAT, Frei C, Goyette S, Halsnaes K, Holt T, Jylhä K, Koffi B, Palutikof J, Schöll R, Semmler T, Woth K (2007) Future extreme events in European climate: an exploration of regional climate model projections. Clim Chang 81:71–95. https://doi.org/10.1007/s10584-006-9226-z

Caloiero T, Veltri S, Caloiero P, Frustaci F (2018) Drought analysis in Europe and in the Mediterranean Basin using the standardized precipitation index. Water 10(8):1043. https://doi.org/10.3390/w10081043

Christensen JH, Christensen OB (2007) A summary of the PRUDENCE model projections of changes in European climate by the end of this century. Clim Chang 81:7–30. https://doi.org/10.1007/s10584-006-9210-7

Conte D and Lionello P. (2019) Effect of model resolution on intense and extreme precipitation over the Mediterranean region (in preparation)

Cramer W, Guiot J, Fader M, Garrabou J, Gattuso J-P, Iglesias A, Lange MA, Lionello P, Llasat MC, Paz S, Peñuelas J, Snoussi M, Toreti A, Tsimplis MN, Xoplaki E (2018) Climate change and interconnected risks to sustainable development in the Mediterranean. Nat Clim Chang 8:972–980. https://doi.org/10.1038/s41558-018-0299-2

Dee DP, Uppala SM, Simmons AJ, Berrisford P, Poli P, Kobayashi S, Andrae U, Balmaseda MA, Balsamo G, Bauer P, Bechtold P, Beljaars ACM, van de Berg L, Bidlot J, Bormann N, Delsol C, Dragani R, Fuentes M, Geer AJ, Haimberger L, Healy SB, Hersbach H, Hólm EV, Isaksen L, Kållberg P, Köhler M, Matricardi M, McNally AP, Monge-Sanz BM, Morcrette J-J, Park B-K, Peubey C, de Rosnay P, Tavolato C, Thépaut J-N Vitart F (2011) The ERA-interim reanalysis: configuration and performance of the data assimilation system. QJR Meteorol Soc 137:553–597. https://doi.org/10.1002/qj.828

Déqué M, Somot S, Sanchez-Gomez E, Goodess CM, Jacob D, Lenderink G, Christensen OB (2012) The spread amongst ENSEMBLES regional scenarios: regional climate models, driving general circulation models and interannual variability. Clim Dyn 38:951–964

Domínguez-Castro F, Vicente-Serrano SM, Tomás-Burguera M, Peña-Gallardo M, Beguería S, El Kenawy A, Luna Y, Morata A (2019) High spatial resolution climatology of drought events for Spain: 1961–2014. Int J Climatol 39:5046–5062. https://doi.org/10.1002/joc.6126

Efthymiadis D, Goodess CM, Jones PD (2011) Trends in Mediterranean gridded temperature extremes and large-scale circulation influences. Nat Hazards Earth Syst Sci 11:2199–2214. https://doi.org/10.5194/nhess-11-2199-2011

Fischer EM, Schär C (2010) Consistent geographical patterns of changes in high-impact European heatwaves. Nat Geosci 3:398–403. https://doi.org/10.1038/ngeo866

Fowler HJ, Ekström M, Blenkinsop S, Smith AP (2007) Estimating change in extreme European precipitation using a multimodel ensemble. J Geophys Res 112:D18104. https://doi.org/10.1029/2007JD008619

García-Herrera R, Garrido-Perez JM, Barriopedro D, Ordóñez C, Vicente-Serrano SM, Nieto R, Gimeno L, Sorí R, Yiou P (2019) The European 2016/17 drought. J Clim 32:3169–3187. https://doi.org/10.1175/JCLI-D-18-0331.1

Gasparrini A, Guo Y, Sera F, Vicedo-Cabrera AM, Huber V, Tong S, de Sousa Zanotti Stagliorio Coelho M, Nascimento Saldiva PH, Lavigne E, Matus Correa P, Valdes Ortega N, Kan H, Osorio S, Kyselý J, Urban A, Jaakkola JJK, Ryti NRI, Pascal M, Goodman PG, Zeka A, Michelozzi P, Scortichini M, Hashizume M, Honda Y, Hurtado-Diaz M, Cruz JC, Seposo X, Kim H, Tobias A, Iñiguez C, Forsberg B, Åström DO, Ragettli MS, Guo YL, Wu CF, Zanobetti A, Schwartz J, Bell ML, Dang TN, Van DD, Heaviside C, Vardoulakis S, Hajat S, Haines A, Armstrong B (2017) Projections of temperature-related excess mortality under climate change scenarios. Lancet Planet Health 1:360-e367. https://doi.org/10.1016/S2542-5196(17)30156-0

Giorgi F, Lionello P (2008) Climate change projections for the Mediterranean region. Glob Planet Chang 63:90–104. https://doi.org/10.1016/j.gloplacha.2007.09.005

Gosling S, Zaherpour J, Mount NJ, Hattermann FF, Dankers R, Arheimer B, Breuer L, Ding J, Haddeland I, Kumar R, Kundu D, Liu J, van Griensven A, Veldkamp TIE, Vetter T, Wang X, Zhang X (2017) A comparison of changes in river runoff from multiple global and catchment-scale hydrological models under global warming

scenarios of 1C, 2C and 3C. Clim Chang 141:577–595. https://doi.org/10.1007/s10584-016-1773-3

Gouveia CM, Trigo RM, Beguería S, Vicente-Serrano SM (2017) Drought impacts on vegetation activity in the Mediterranean region: an assessment using remote sensing data and multi-scale drought indicators. Glob Planet Chang 151:15–27

Grillakis M (2019) Increase in severe and extreme soil moisture droughts for Europe under climate change. Sci Total Environ 660:1245–1255

Hertig E, Tramblay Y (2017) Regional downscaling of Mediterranean droughts under past and future climatic conditions. Glob Planet Chang 151:36–48

Hertig E, Seubert S, Jacobeit J (2010) Temperature extremes in the Mediterranean area: trends in the past and assessments for the future. Nat Hazards Earth Syst Sci 10:2039–2050. https://doi.org/10.5194/nhess-10-2039-2010

Hochman A, Mercogliano P, Alpert P, Saaroni H, Bucchignani E (2018) High-resolution projection of climate change and extremity over Israel using COSMO-CLM. Int J Climatol 38:5095–5106. https://doi.org/10.1002/joc.5714

Jacob D, Petersen J, Eggert B, Alias A, Christensen OB, Bouwer LM, Braun A, Colette A, Déqué M, Georgievski G, Georgopoulou E, Gobiet A, Menut L, Nikulin G, Haensler A, Hempelmann N, Jones C, Keuler K, Kovats S, Kröner N, Kotlarski S, Kriegsmann A, Martin E, van Meijgaard E, Moseley C, Pfeifer S, Preuschmann S, Radermacher C, Radtke K, Rechid D, Rounsevell M, Samuelsson P, Somot S, Soussana JF, Teichmann C, Valentini R, Vautard R, Weber B, Yiou P (2014) EURO-CORDEX: new high-resolution climate change projections for European impact research. Reg Environ Chang 14:563–578

Kalnay E, Kanamitsu M, Kistler R, Collins W, Deaven D, Gandin L, Iredell M, Saha S, White G, Woollen J, Zhu Y, Leetmaa A, Reynolds B, Chelliah M, Ebisuzaki W, Higgins W, Janowiak J, Mo KC, Ropelewski C, Wang J, Jenne R, Joseph D (1996) The NCEP/NCAR 40-Year Reanalysis Project. Bulletin of the American. Meteorol Soc 77(3):437–472. https://doi.org/10.1175/1520-0477(1996)077<0437:TNYRP>2.0.CO;2

Kendrovski V, Baccini M, Martinez GS, Wolf T, Paunovic E, Menne B (2017) Quantifying Projected Heat Mortality Impacts under 21st-Century Warming Conditions for Selected European Countries. Int. J. Environ. Res. Public Health 14:729.

Kistler R, Kalnay E, Collins W, Saha S, White G, Woollen J, Chelliah M, Ebisuzaki W, Kanamitsu M, Kousky V, van den Dool H, Jenne R, Fiorino M (2001) The NCEP–NCAR 50-year reanalysis: Monthly means CD-ROM and documentation. Bull. Am. Meteorol. Soc. 82: 247–267.

Koutroulis AG, Papadimitriou LV, Grillakis MG, Tsanis IK, Wyser K, Betts RA (2018) Freshwater vulnerability under high end climate change. A pan-European assessment. Sci Total Environ 13:271–286

Kovats RS, Valentini R, Bouwer LM, Georgopoulou E, Jacob D, Martin E, Rounsevell M, Soussana JF (2014) Europe. In: Barros VR, Field CB, Dokken DJ, Mastrandrea MD, Mach KJ, Bilir TE, Chatterjee M, Ebi KL, Estrada YO, Genova RC, Girma B, Kissel ES, Levy AN, MacCracken S, Mastrandrea PR, White LL (eds) Climate Change 2014: Impacts, Adaptation, and Vulnerability. Part B: Regional Aspects. Contribution of Working Group II to the Fifth Assessment Report of the Intergovernmental Panel on ClimateChange. Cambridge University Press, Cambridge, pp 1267–1326

Kuglitsch FG, Toreti A, Xoplaki E, Della-Marta PM, Zerefos CS, Türkeş M, Luterbacher J (2010) Heat wave changes in the eastern Mediterranean since 1960. Geophys Res Lett 37:L04802. https://doi.org/10.1029/2009GL041841

Lehner F, Coats S, Stocker TF, Pendergrass AG, Sanderson BM, Raible CC, Smerdon JE (2017) Projected drought risk in 1.5°C and 2°C warmer climates. Geophys Res Lett 44:7419–7428. https://doi.org/10.1002/2017GL074117

Lelieveld J, Proestos Y, Hadjinicolaou P, Tanarhte M, Tyrlis E, Zittis G (2016) Strongly increasing heat extremes in the Middle East and North Africa (MENA) in the 21st century. Clim Chang 137:245–260. https://doi.org/10.1007/s10584-016-1665-6

Lionello P, Scarascia L (2018) The relation between climate change in the Mediterranean region and global warming. Reg Environ Chang 18: 1481–1493. https://doi.org/10.1007/s10113-018-1290-1

Lionello P, Abrantes F, Congedi L, Dulac F, Gacic M, Gomis D, Goodess C, Hoff H, Kutiel H, Luterbacher J, Planton S, Reale M, Schröder K, Struglia M V, Toreti A, Tsimplis M, Ulbrich U, Xoplaki E (2012) Introduction: Mediterranean climate: background information in Lionello P (Ed.) The Climate of the Mediterranean Region. From the Past to the Future, Amsterdam: Elsevier (NETHERLANDS), xxxv-xc, ISBN: 9780124160422, doi: https://doi.org/10.1016/B978-0-12-416042-2.00012-4

Llasat MC, Llasat-Botija M, Prat MA, Porcú F, Price C, Mugnai A, Lagouvardos K, Kotroni V, Katsanos D, Michaelides S, Yair Y, Savvidou K, Nicolaides K (2010) High-impact floods and flash floods in Mediterranean countries: the FLASH preliminary database. Adv Geosci 23:47–55. https://doi.org/10.5194/adgeo-23-47-2010

Mathbout S, Lopez-Bustins JA, Royé D, Martin-Vide J, Bech J, Rodrigo FS (2018) Observed changes in daily precipitation extremes at annual timescale over the eastern Mediterranean during 1961-2012. Pure Appl Geophys 175:3875–3890. https://doi.org/10.1007/s00024-017-1695-7

Miralles DG, Gentine P, Seneviratne SI, Teuling AJ (2019) Land-atmospheric feedbacks during droughts and heatwaves: state of the science and current challenges. Ann N Y Acad Sci 1436:19–35. https://doi.org/10.1111/nyas.13912

Nakićenović R, Alcamo NJ, Davis G, de Vries B, Fenhann J, Gaffin S, Gregory K, Grübler A, Jung TY, Kram T, La Rovere EL, Michaelis L, Mori S, Morita T, Pepper W, Pitcher H, Price L, Raihi K, Roehrl A, Rogner HH, Sankovski A, Schlesinger M, Shukla P, Smith S, Swart R, van Rooijen S, Victor N, Dadi Z (2000) IPCC special report on emissions scenarios. Cambridge University Press, Cambridge, 599pp

Naumann G, Alfieri L, Wyser K, Mentaschi L, Betts RA, Carrao H, Spinoni J, Vogt J, Feyen L (2018) Global changes in drought conditions under different levels of warming. Geophys Res Lett 4: 3285–3296. https://doi.org/10.1002/2017GL076521

Paravantis J, Santamouris M, Cartalis C, Efthymiou C, Kontoulis N (2017) Mortality associated with high ambient temperatures, heatwaves, and the urban heat island in Athens, Greece. Sustainability 9:606. https://doi.org/10.3390/su9040606

Paz S, Negev M, Clermont A, Green MS (2016) Health aspects of climate change in cities with Mediterranean climate, and local adaptation plans. Int J Environ Res Public Health 13:438. https://doi.org/10.3390/ijerph13040438

Peñuelas J, Sardans J, Filella I, Estiarte M, Llusià J, Ogaya R, Carnicer J, Bartrons M, Rivas-Ubach A, Grau O, Peguero G, Margalef O, Pla-Rabés S, Stefanescu C, Asensio D, Preece C, Liu L, Verger A, Barbeta A, Achotegui-Castells A, Gargallo-Garriga A, Sperlich D, Farré-Armengol G, Fernández-Martínez M, Liu D, Zhang C, Urbina I, Camino-Serrano M, Vives-Ingla M, Stocker BD, Balzarolo M, Guerrieri R, Peaucelle M, Marañón-Jiménez S, Bórnez-Mejías K, Mu Z, Descals A, Castellanos A, Terradas J (2017) Impacts of global change on Mediterranean forests and their services. Forests 8:463

Planton S, Lionello P, Artale V, Aznar R, Carrillo A, Colin J, Congedi L, Dubois C, Elizalde A, Gualdi S, Hertig E, Jacobeit J, Jordà G, Li L, Mariotti A, Piani C, Ruti P, Sanchez-Gomez E, Sannino G, Sevault F, Somot S, Tsimplis M (2012) The climate of the Mediterranean region in future climate. In: Lionello P (ed) The Climate of the Mediterranean Region. From the Past to the Future. Elsevier (NETHERLANDS), Projections, Amsterdam, pp 449–502. https://doi.org/10.1016/B978-0-12-416042-2.00008-2

Pumo D, Caracciolo D, Viola F, Noto LV (2016) Climate change effects on the hydrological regime of small non-perennial river basins. Sci Total Environ 542:76–92

Ruti P, Somot S, Giorgi F, Dubois C, Flaounas E, Obermann A, Dell'Aquila A, Pisacane G, Harzallah A, Lombardi E, Ahrens B, Akhtar N, Alias A, Arsouze T, Raznar R, Bastin S, Bartholy J, Beranger K, BeuvierJ B-CS, Brauch J, Cabos W, Calmanti S, Calvet JC, Carillo A, Conte D, Coppola E, Djurdjevic V, Drobinski P, Elizalde A, Gaertner M, Galan P, Gallardo C, Gualdi S, Goncalves M, JorbaO JG, Lhevede B, Lebeaupin-Brossier C, Li L, Liguori G, Lionello P, Macias-Moy D, Onol B, Rajkovic B, RamageK SF, Sannino G, Struglia MV, Sanna A, Torma C, Vervatis V, Nabat P (2015) Med-CORDEX initiative for Mediterranean climate studies. Bull Am Meteorol Soc 97:1187–1208. https://doi.org/10.1175/BAMS-D-14-00176.1

Samuels R, Hochman A, Baharad A, Givati A, Levi Y, Yosef Y, Saaroni H, Ziv B, Harpaz T, Alpert P (2018) Evaluation and projection of extreme precipitation indices in the eastern Mediterranean based on CMIP5 multi-model ensemble. Int J Climatol 38:2280–2297. https://doi.org/10.1002/joc.5334

Scoccimarro E, Gualdi S, Bellucci A, Zampieri M, Navarra A (2016) Heavy precipitation events over the Euro-Mediterranean region in a warmer climate: results from CMIP5 models. Reg Environ Change 16:595–602 (2016). https://doi.org/10.1007/s10113-014-0712-y

Sillmann J, Kharin VV, Zhang X, Zwiers FW, Bronaugh D (2013a) Climate extremes indices in the CMIP5 multimodel ensemble: part 1. Model evaluation in the present climate. J Geophys Res Atmos 118:1716–1733. https://doi.org/10.1002/jgrd.50203

Sillmann J, Kharin VV, Zhang X, Zwiers FW, Bronaugh D (2013b) Climate extremes indices in the CMIP5 multimodel ensemble: part 2. Future climate projections. J Geophys Res Atmos 118:2473–2493. https://doi.org/10.1002/jgrd.50188

Spinoni J, Vogt JV, Naumann G, Barbosa P, Dosio A (2018) Will drought events become more frequent and severe in Europe? Int J Climatol 38:1718–1736. https://doi.org/10.1002/joc.5291

Spinoni J, Barbosa P, De Jager A, McCormick N, Naumann G, Vogt V, Magni J, Masante D, Mazzeschi D (2019) A new global database of meteorological drought events from 1951 to 2016. J Hydrol Reg Stud 22:100593. https://doi.org/10.1016/j.ejrh.2019.100593

Stagge JH, Kingston DG, Tallaksen LM, Hannah DM (2017) Observed drought indices show increasing divergence across Europe. Sci Rep 7(1):14045. https://doi.org/10.1038/s41598-017-14283-2

Taylor KE, Stouffer RJ, Meehl GA (2012) An overview of CMIP5 and the experiment design. Bull Am Meteorol Soc 93(4):485–498. https://doi.org/10.1175/BAMS-D-11-00094.1

Tramblay Y, Somot S (2018) Future evolution of extreme precipitation in the Mediterranean. Clim Chang 151:289–302. https://doi.org/10.1007/s10584-018-2300-5

Turco M, von Hardenberg J, AghaKouchak A, Llasat MC, Provenzale A, Ricardo M, Trigo RM (2017) On the key role of droughts in the dynamics of summer fires in Mediterranean Europe. Sci Rep 7:81. https://doi.org/10.1038/s41598-017-00116-9

Ulbrich U, Lionello P, Belušic D, Jacobeit J, Knippertz P, Kuglitsch FG, Leckebusch GC, Luterbacher J, Maugeri M, Maheras P, Nissen KM, Pavan V, Pinto JG, Saaroni H, Seubert S, Toreti A, Xoplaki E, Ziv B (2012) Climate of the Mediterranean: synoptic patterns, temperature, precipitation, winds, and their extremes. In: Lionello P (ed) The Climate of the Mediterranean Region. From the Past to the Future. Elsevier (NETHERLANDS), Amsterdam, pp 301–346, ISBN:9780124160422. https://doi.org/10.1016/b978-0-12-416042-2.00005-7

Uppala SM, KÅllberg PW, Simmons AJ, Andrae U, Bechtold VD, Fiorino M, Gibson JK, Haseler J, Hernandez A, Kelly GA, Li X, Onogi K, Saarinen S, Sokka N, Allan RP, Andersson E, Arpe K, Balmaseda MA, Beljaars AC, Berg LV, Bidlot J, Bormann N, Caires S, Chevallier F, Dethof A, Dragosavac M, Fisher M, Fuentes M, Hagemann S, Hólm E, Hoskins BJ, Isaksen L, Janssen PA, Jenne R, Mcnally AP, Mahfouf J, Morcrette J, Rayner NA, Saunders RW, Simon P, Sterl A, Trenberth KE, Untch A, Vasiljevic D, Viterbo P, Woollen J (2005) The ERA-40 re-analysis. QJR Meteorol Soc 131:2961–3012. https://doi.org/10.1256/qj.04.176

Vicente-Serrano SM, Lopez-Moreno JI, Beguería S, Lorenzo-Lacruz J, Sanchez-Lorenzo A, García-Ruiz JM, Azorin-Molina C, Tejeda-Moran E, Revuelto J, Trigo R, Coelho F, Espejo F (2014) Evidence of increasing drought severity caused by temperature rise in southern Europe. Environ Res Lett 9:044001. https://doi.org/10.1088/1748-9326/9/4/044001

Vicente-Serrano SM, Van der Schrier G, Beguería S, Azorin-Molina C, Lopez-Moreno JI (2015) Contribution of precipitation and reference evapotranspiration to drought indices under different climates. J Hydrol 526:42–54

Vicente-Serrano SM, Lopez-MorenoJI BS, Lorenzo-Lacruz J, Sanchez-Lorenzo A, García-Ruiz JM, Azorin-Molina C, Morán-Tejeda E, Revuelto J, Trigo R, Coelho F, Espejo F (2019) Evidence of increasing drought severity caused by temperature rise in southern Europe. Environ Res Lett 9:044001. https://doi.org/10.1088/1748-9326/9/4/044001

Wanders N, Wada Y, Van Lanen HAJ (2015) Global hydrological droughts in the 21st century under a changing hydrological regime. Earth Syst Dynam 6:1–15. https://doi.org/10.5194/esd-6-1-2015

Zittis G, Hadjinicolaou P, Fnais M, Lelieveld J (2016) Projected changes in heat wave characteristics in the eastern Mediterranean and the Middle East. Reg Environ Chang 16:1863–1876. https://doi.org/10.1007/s10113-014-0753-2

Zollo AL, Rillo V, Bucchignani E, Montesarchio M, Mercogliano P (2016) Extreme temperature and precipitation events over Italy: assessment of high-resolution simulations with COSMO-CLM and future scenarios. Int J Climatol 36:987–1004. https://doi.org/10.1002/joc.4401